

Modelling of storage tanks with immersed heat exchangers

J. Cadafalch^{a,*}, D. Carbonell^{b,1}, R. Cònsul^a, R. Ruiz^a

^a*Universitat Politècnica de Catalunya BarcelonaTech (UPC), Green Technologies
Research Group (GreenTech), Terrassa, Spain.*

^b*RDmes Technologies S.L., Ctra. Nac. 150, km 14.5, Institut Politècnic, 08227
Terrassa, Spain.*

Abstract

A model of a storage tank with an immersed serpentine heat exchanger is described and validated against experimental data available from the literature. The tank is modelled one dimensionally using the multi-node approach corrected by an energy conservative reversion elimination algorithm to prevent inverse gradient solutions to occur. A one dimensional model in the flow direction is also used for the serpentine based on control volume techniques. The serpentine is discretized in equal sized control volumes and the energy equation is solved in each of them. The energy exchanged between the serpentine and the tank is then introduced as an internal heat source of the tank multi-node. With this model the behaviour of tanks with internal serpentine can be predicted minimizing tuning parameters to be derived from previous experimental analysis of the tank. Additionally, by an appropriate formulation of the governing equations in the serpentine control volumes, it is possible to handle complex internal fluid phenomena as coupling of the tank within a thermosyphon cycle or two phase flow.

Keywords:

Storage tanks, Modelling, Serpentine, Immersed heat exchanger

*Corresponding author

Email address: jcadafalch@mmt.upc.edu (J. Cadafalch)

¹Present address: SPF Institut für Solartechnik, Hochschule für Technik (HSR), CH-8640 Rapperswil, Switzerland.

1
2
3
4
5
6
7
8
9 **1. Introduction**

10
11 In most solar thermal systems some kind of heat exchanger is used to
12 separate the thermal fluid circulating through the collector field from the
13 thermal fluid inside the tank. For medium or small size systems, with a
14 store volume below around 2000 l, the heat exchanger is normally integrated
15 within the tank. Mantle tanks or storages with immersed heat exchangers
16 are the two main devices used for this purpose.
17

18
19 Mantle tanks, also known as jacket or annular heat exchangers, are the
20 simplest and cheapest means of obtaining high thermal effectiveness while
21 promoting stratification. However, as discussed by Furbo (1993) and Shah
22 (2000), the use of mantle tanks is limited to volumes below 800-1000 l, be-
23 cause above these volumes heat transfer area reduces considerably. In tanks
24 with immersed heat exchangers this problem is overcome. Additionally, the
25 tank to ambient heat loss coefficient is also reduced.
26
27

28 Three and two dimensional models for storage tanks can be used to inves-
29 tigate specific phenomena. For example, the thermal stratification of cylin-
30 drical horizontal tanks has recently been analysed by Savicki et al. (2011);
31 and Yan Su et al. (2008) studied the transient heat transfer characteris-
32 tics of immersed serpentine heat exchangers. From these studies, very de-
33 tailed information can be obtained. However, the computational demand is
34 high, and the model must be run by specialists. As a consequence, they are
35 not suitable for long term studies under operation conditions and cannot be
36 used in market-oriented solar thermal systems engineering. Therefore, one-
37 dimensional tank approaches are still normally used for long term studies as
38 those recently presented by Campos Celador et al. (2011), Young-Deuk Kim
39 et al. (2012), Banister et al. (2014) or Shuhong Li et al. (2014), because they
40 are able to offer an optimal compromise between accuracy and computational
41 effort.
42
43
44
45

46 A widely used one-dimensional model for storage tanks is the multi-node
47 model developed by Kleinbach et al. (1993). The tank is divided in different
48 nodes from the bottom to the top, and the energy and mass conservation
49 equations are solved at each of them over the time. This results into a one
50 dimensional transient resolution of the tank.
51

52 An extension of the multi-node model was proposed by Newton et al.
53 (1995) to include an immersed heat exchanger. This model assumes a con-
54 stant heat transfer coefficient between the heat exchanger and storage fluid
55 that must be introduced as an input value.
56
57
58

1
2
3
4
5
6
7
8
9 A multi-port store model able to include four immersed heat exchangers
10 was developed by Druck et al. (1994). The heat transfer coefficient must also
11 be introduced by the user for specific conditions. Therefore, experimental
12 data should be used to estimate this parameter, what is known as model
13 tuning process. Time dependence of the heat transfer coefficient is then
14 directly estimated by the model. This model is widespread in solar ther-
15 mal system testing. However, the experimental data required for the tuning
16 process is not always available for commercial stores.

17
18
19 Additionally, the multi-node model for storage tanks must also include
20 a reversion elimination algorithm, see Mather et al. (2002). Basically, this
21 algorithm forces that fluid temperatures of the different layers increase with
22 height. When the storage tank is heated in positions different from the
23 top, a positive density vertical gradient provoke a fluid instability, which in
24 turns causes a mixing process due to natural convection. This process ends
25 up with a uniformly mixed temperature in the upper layers. The multi-
26 node model is not able to directly solve the instantaneous highly convective
27 phenomena that takes places. The reversion elimination algorithm overcomes
28 this problem. The work presented by Newton et al. (1995) describes this
29 algorithm. Basically the idea is to check if there exists a layer with higher
30 temperature than its upper neighbour. If this occurs, the two layers are
31 mixed. The problem here relies in how the layers are mixed. From the
32 author's knowledge, a volumetric mixing process is chosen for most of the
33 models, see for example the models of Newton et al. (1995) and Druck et al.
34 (1994).

35
36
37 In this paper, a model for storage tanks with immersed serpentine heat
38 exchangers is presented. The model does not need a previous tuning process
39 for the serpentine, and includes an energy conservative reversion elimination
40 mechanism. The serpentine is discretized in different control volumes in the
41 fluid flow direction. The energy equation is then solved for each of them. The
42 convective heat transfer coefficients in the inner fluid and from the serpentine
43 walls to the store, are calculated from empirical correlations. With this
44 approach, if an appropriate governing equations formulation is used inside the
45 serpentine heat exchanger, the model can also be extended to more complex
46 heat transfer analysis, as coupling of the serpentine within a thermosyphone
47 loop, or use of phase change fluid in the serpentine, for example when a heat
48 pump condenser is integrated in the storage tank.

49
50
51 The mathematical formulation and numerical resolution of the model is
52 explained in the following section. Afterwards, a comparison of numerical
53
54
55
56
57
58

1
2
3
4
5
6
7
8
9 results with experimental data available in the literature for two different
10 test cases are presented in order to assess credibility to the model.
11

12 2. Mathematical formulation

13 2.1. Modified multi-node

14
15 The multi-node model for stratified storage tanks as described in Klein-
16 bach et al. (1993) is used coupled with an immersed heat exchanger model.
17

18 The tank is divided into N equal sized control volumes in the vertical
19 direction called nodes. They are numbered from the bottom to the top,
20 being $n = 1$ the node at the bottom, and $n = N$ the node at the top of
21 the tank. A single node assumes fully mixed tank, and increased number of
22 nodes results into a more stratified tank.
23

24 The energy and mass conservation law is then solved at each node.
25

26 For simplicity, the formulation presented hereafter addresses a tank with
27 a single immersed heat exchanger connected to a collector field loop, and a
28 single draw-off loop.
29

30 The energy equation at a generic node n according to the multi-node
31 model reads as follows:
32

$$33 \dot{Q}_n^{accum} + \dot{Q}_n^{loss} + \dot{Q}_n^{mix} = \dot{Q}_n^{col} - \dot{Q}_n^{load} \quad (1)$$

34 The term \dot{Q}_n^{accum} is the accumulated heat at the node in W. Using a first
35 order scheme for the time derivatives, and a time increment of Δt , this term
36 is evaluated as a function of the temperature of the node at the current time
37 step T_n and the temperature of the node at the previous time step T_n^o as:
38
39
40

$$41 \dot{Q}_n^{accum} = \rho_n c_{p_n} V_n \frac{T_n - T_n^o}{\Delta t} \quad (2)$$

42 where c_{p_n} and ρ_n are the storage fluid heat capacity and density, and V_n
43 the volume of the node.
44

45 The heat losses to ambient in Eq. 1 is represented as \dot{Q}_n^{loss} and can be
46 computed in terms of the ambient temperature T^a and the node to ambient
47 overall heat transfer coefficient UA_n^{loss} :
48
49
50

$$51 \dot{Q}_n^{loss} = UA_n^{loss} (T_n - T^a) \quad (3)$$

52 The node to ambient heat transfer coefficient UA_n^{loss} can be approximated
53 multiplying the overall tank heat loss coefficient, UA^{tnk} , by the fraction of
54 the tank external area that belongs to the analysed node:
55
56
57

$$\dot{U}A_n^{loss} = UA^{tnk} \frac{S_n^a}{A^{tnk}} \quad (4)$$

where S_n^a is the surface contact area between the node n and the ambient.

Mixing effects between neighbouring nodes is considered by means of \dot{Q}_n^{mix} . This term makes use of an equivalent conductivity coefficient Λ that represents the level of mixing of the tank in stand by conditions (when there is not energy exchange with the collector and load loop). The Λ coefficient accounts for thermal conductivity of the storage fluid, and for internal free convective phenomena that may occur due to the presence of thermal bridges in the walls or internal elements. Accordingly, the mixing term, is then calculated as a function of the nodes temperatures as follows:

$$\dot{Q}_n^{mix} = \frac{\Lambda}{\delta_{n+1}} S_n^{n+1} (T_n - T_{n+1}) + \frac{\Lambda}{\delta_{n-1}} S_n^{n-1} (T_n - T_{n-1}) \quad (5)$$

where T_{n+1} and T_{n-1} are the top and bottom neighbour nodes, δ_{n+1} and δ_{n-1} the distance between the centre of the node and the center of the neighbour nodes, and S_n^{n+1} and S_n^{n-1} the node surface in contact with the neighbouring nodes. In case of vertical cylindrical tank, these two surfaces are identical. In other tank geometries such as horizontal tanks, these two surfaces may differ.

The two terms on the right in the energy balance as represented in Eq. 1, are the energy introduced at the node from the collector loop \dot{Q}_n^{col} and the energy removed to the load loop \dot{Q}_n^{load} . The energy removed by the load loop, is calculated from an enthalpy balance using an upwind scheme for the temperatures. Accordingly, it is evaluated as follows:

$$\dot{Q}_n^{load} = \dot{m}^{load} c_{p_n} (T_n - T_n^{load}) \quad (6)$$

where \dot{m}^{load} is the instantaneous load mass flow rate, and T_n^{load} the temperature of the fluid entering the node. In the nodes where the loop inlet is placed, this temperature takes the value of the inlet fluid flow temperature. In other nodes, it takes the value of the lower node T_{n-1} .

As in the standard multi-node model direct fluid exchange in the collector loop is assumed, the term \dot{Q}_n^{col} in Eq. 1 is calculated using a similar procedure to that used for the load term \dot{Q}_n^{load} . To account for the effect of the immersed heat exchanger in the collector loop, \dot{Q}_n^{col} is calculated from the immersed heat exchanger model described in subsection 2.2. This term is then renamed as:

$$\dot{Q}_n^{col} = \dot{Q}_n^{hx} \quad (7)$$

By applying the formulation given above, a set of algebraic equations (one for each node) is obtained being the temperature of the nodes at the current time step the unknowns. For an intermediate node the algebraic equation reads:

$$A_n^o T_n^o + A_n T_n + A_{n+1} T_{n+1} + A_{n-1} T_{n-1} + (B + \dot{Q}_n^{hx}) = 0 \quad (8)$$

As the algebraic coefficients A and B and the term \dot{Q}_n^{hx} may depend on the nodes temperatures, the algebraic equation set is not linear. A iterative solver based on tridiagonal matrix algorithm is used to solve the resulting equations system, Patankar (1980).

2.2. Immersed heat exchanger

The serpentine immersed heat exchanger is evaluated with a step-by-step model as describer by Carbonell et al. (2013). The temperature of the fluid inside the serpentine is calculated by means of a one-dimensional analysis in the fluid flow direction applying a control volume discretization technique. The serpentine is discretized in M equal sized control volumes and the energy equation is solved at each of them, see Fig. 1. For convenience, the fluid temperatures are evaluated at the surfaces of the control volumes in the flow direction, and the temperature of the control volume is calculated from an averaging of the two corresponding temperatures. The calculated temperatures are represented by T_m being T_1 and T_{M+1} the temperature of the fluid at the inlet and outlet of the heat exchanger respectively. The average temperature of the control volume m , is then represented by \overline{T}_m , and is calculated as the average of T_m and T_{m+1} . Accordingly, the energy equation at a control volume m using a first order scheme for the time derivatives, and neglecting the heat axial conduction and the energy accumulation at the pipe walls, reads as follows:

$$\rho c_p V \frac{\overline{T}_m - \overline{T}_m^o}{\Delta t} + \dot{m} c_p (T_{m+1} - T_m) + U A_m^{hx} (\overline{T}_m - T_{m_{ext}}) = 0 \quad (9)$$

where the superscript o in \overline{T}_m^o refers to the value at the previous computed time step, ρ and c_p are the density and specific heat of the inner fluid, \dot{m} is the inner mass flow rate, V the volume of fluid contained in the control volume, $U A_m^{hx}$ is the heat transfer coefficient from the inner fluid to the external fluid

and $T_{m_{ext}}$ is the temperature of the external fluid, i.e. the temperature of the tank node n in which the serpentine control volume m is placed.

The M algebraic equations resulting from the discretized energy conservation law, Eq. 9, are solved following a step by step procedure (from the inlet to the outlet). The model needs no iterations if physical properties and UA_m are calculated from the inlet fluid temperature T_m for each control volume. The heat transferred from the serpentine to the tank node n , \dot{Q}_n^{hx} , is finally calculated from the summation of the heat loss term of all serpentine control volumes CVs placed inside the tank node n as follows:

$$\dot{Q}_n^{hx} = \sum^{CVs} UA_m^{hx} (\overline{T}_m - T_n) \quad (10)$$

2.2.1. Heat transfer coefficient UA_m^{hx}

The heat transfer coefficient from the serpentine internal fluid to the tank node fluid, is calculated according to the standard formulation of heat transfer through a cylindrical wall:

$$UA_m^{hx} = \left[\frac{D_{ext}}{h_{int} D_{int}} + \frac{1}{\kappa^{wall}} + \frac{1}{h_{m_{ext}}} \right]^{-1} A_{m_{ext}} \quad (11)$$

where D_{ext} and $A_{m_{ext}}$ are the external diameter and area of the pipe, D_{int} means the internal diameter of the pipe, κ^{wall} is the conductance of the pipe wall, and $h_{m_{ext}}$ and h_{int} the external and internal convective heat transfer coefficient of the pipe control volume m .

The pipe wall conductance is calculated referred to the external pipe area, and depends on the wall conductivity λ^{wall} and the external and internal pipe diameters according to the following equation:

$$\kappa^{wall} = \frac{\lambda^{wall}}{\frac{D_{ext}}{2} \ln \frac{D_{ext}}{D_{int}}} \quad (12)$$

The internal convective heat transfer coefficient h_{int} , is obtained from experimental correlations of the Nusselt number for forced convective heat transfer fluid flow through cylindrical tubes as reported in Wong (1977), as a function of the Reynold and Prandtl dimensionless numbers:

$$\frac{h_{int} D_{int}}{\lambda_{int}} = Nu_{int} = C Re^m Pr^n K \quad (13)$$

where λ_{int} is the thermal conductivity of the inner fluid, D_{int} the inner tube diameter, and the coefficients C , m, n and K depend on the flow regime, and the tube length, see Table 1.

The external convective heat transfer coefficient at the serpentine control volume m $h_{m_{ext}}$ is calculated according to the expression of combined free and forced convection around immersed bodies described by Churchill (2002). The external Nusselt number at the control volume m $Nu_{m_{ext}}$ is calculated as the average of two Nusselts labelled with the super indexes + and -, which are calculated from a function combining the free (natural) convective Nusselt number Nu_m^N and the forced convective Nusselt number Nu_m^F . The formulation is able to handle both positive (heating) and negative (cooling) heat transfer from the serpentine to the tank. Accordingly, $Nu_{m_{ext}}$ is calculated with the following equation:

$$\frac{h_{m_{ext}} \pi D_{ext}}{\lambda} = Nu_{m_{ext}} = \frac{Nu_m^+ + Nu_m^-}{2} \quad (14)$$

where Nu^+ and Nu^- are obtained from the functions of the natural and forced convective Nusselt numbers:

$$\begin{aligned} Nu_m^- &= 1 + |(Nu_m^F)^4 - (Nu_m^N)^4|^{\frac{1}{4}} \\ Nu_m^+ &= 1 + |(Nu_m^F)^4 + (Nu_m^N)^4|^{\frac{1}{4}} \end{aligned} \quad (15)$$

The forced Nusselt Nu_m^F is obtained from:

$$Nu_m^F = A_F Re_m^{1/2} Pr_m^{1/3} [1 + (C_F / Pr_m)^{2/3}]^{-1/4} \quad (16)$$

where Re_m and Pr_m are the Reynolds and Prandtl number respectively. The coefficients A_F and C_F are obtained as a function of the shape and boundary conditions. For a horizontal cylinder with uniform temperature (the closest approach) $A_F = 1.08$ and $C_F = 0.412$. The Reynolds number Re_m is calculated using the tank fluid physical properties, the average velocity of the fluid circulating through the node in which the serpentine control volume m is placed, and πD_{ext} as characteristic length.

The natural Nusselt number at the serpentine control volume m is obtained from a general expression proposed by Farrington et al. (1986):

$$Nu_m^N = C_N (Gr_m Pr_m)^{n_N} \quad (17)$$

where the coefficients C_N and n_N are user defined. Farrington et al. (1986) suggested to fit this values with experimental data. However, as addressed by Newton et al. (1995) if this data is not available, the values of $C_N = 0.5$ and $n_N = 0.25$ can be used. The Prandtl and Grashof numbers Pr_m and Gr_m in Eq. 17 are calculated using the tank fluid physical properties of the corresponding node. The equation for Gr_m reads as follows:

$$Gr_m = \frac{g\beta\rho^2 \left| \overline{T_m^{wall}} - T_{m_{ext}} \right| (\pi D_{ext})^3}{\mu^2} \quad (18)$$

where $\overline{T_m^{wall}}$ is the wall temperature of the serpentine control volume m and $T_{m_{ext}}$ the temperature of the corresponding tank node.

2.3. Tuning parameters

Beside geometrical parameters of the tank and the serpentine, the model requires some further information that can be obtained from experiments following standard procedures defined in EN 12977-3 (2012), or from a numerical evaluation of the tank with higher level numerical tools as for example is described in the work of Consul et al. (2004). Main parameters are the number of nodes to be used in the multi-node model N , the tank ambient heat loss coefficient UA^{tnk} and the value of the coefficients to account for the effective conductive heat transfer between the nodes Λ .

To better predict the performance of the serpentine, the values C_N and n_N from Eq. 17 can also be adjusted from experimental data of the performance of the serpentine under different working conditions. However, such experimental data is usually not available for commercial storage tanks. In these cases, the standard values as discussed in Section 2.2.1 can be used, i.e. $C_N=0.5$ and $n_N=0.25$.

2.4. Reversion elimination algorithm

When a tank is heated up by means of a immersed heat exchanger placed at its bottom, negative density gradients may occur. As a consequence, a fluid motion is generated which in turns produces a fast mixing. The mixing process ends with a uniform temperature of the tank section above where the density gradient was present.

A detailed modelling of this phenomena can be carried out by direct resolution of the transient Navier-Stokes Equations for free-convection in

1
2
3
4
5
6
7
8
9 order to take into account the different temporal and spacial characteristic
10 scales.

11 The multi-node model approach, which is based in global energy and
12 mass balances at the different nodes distributed vertically, may result into
13 unrealistic temperature inversions when the tank is being heated up by a
14 heat exchanger placed at its bottom. A so called reversion elimination algo-
15 rithm for multi-node model was suggested by Newton et al. (1995) in order
16 overcome this problem. Once mass and energy equation at each node are
17 solved, a routine consisting of running through all the tank nodes from the
18 top to the bottom is applied. If the temperature below the analysed node
19 is higher, then the two nodes are mixed. If this temperature is still lower
20 than the next node, the three are mixed. The procedure continues until a
21 node with lower temperature is found. This algorithm is repeated until the
22 criteria of $T_n \geq T_{n-1}$ is fulfilled for all nodes. A key aspect of the method
23 relies on how the temperature of the nodes involved in the process explained
24 above are mixed.
25
26
27
28
29

30 A reversion elimination algorithm based on energy conservation is here
31 presented.

32 Mixing process is achieved by setting the equivalent conductivity coeffi-
33 cient between the mixed nodes Λ in Eq. 5, to infinity. This numerical trick
34 results into zero temperature gradient solution between the mixed nodes.
35

36 For each simulated time step, the set of algebraic energy equations, see
37 Eq. 8, is solved sequentially as times as necessary until temperature reversion
38 is eliminated. The first computation is performed by using the Λ physical
39 values of the tank (according to the input data). After the first computation
40 is finished, all Λ values between those nodes with inverse temperatures are set
41 to infinity, and the set of algebraic equations are solved for a second time.
42 The Λ coefficients between the nodes to be mixed is then kept to a value
43 of infinity until the final time step solution is reached. As the solution of
44 the second computation may also contain some temperature inversions, the
45 procedure is carried out again. This procedure is repeated until no inverse
46 temperatures are found. The total number of computations to achieve none-
47 inverse temperature solutions ranges from 1, in those cases where there is no
48 inversion, to N (being N the number of nodes used in the multi-node
49 model), in those cases with maximum inverse temperature distribution.
50
51
52
53
54
55
56
57
58
59
60
61
62
63
64
65

3. Results

Two different cases are used to validate the model. They both consist of a tank with an immersed serpentine heat exchanger placed at its bottom which introduces or removes energy from the tank following different patterns. Numerical results obtained with the methodology here described are validated by comparison to experimental data reported by Farrington et al. (1986) and Mather et al. (2002). Results are presented in figures reproducing the reporting criteria adopted by these authors to present their experimental data.

Computations here not reported have been carried out in order to investigate the sensitivity of the output analysed data on the discretization parameters M (number of control volumes in the serpentine) and Δt . The parameter M was varied from 5 to 1000, and the value of Δt from 15 to 450 s. No significant differences were found in any case. Therefore, all numerical results here presented have been obtained with a Δt of 450 s and with 5 control volumes in the serpentine in order to save computational effort.

The parameters that have been tuned to match the experiments are indicated in Table 2. Details of the tanks and heat exchangers geometry and discretization are shown in Fig. 2.

3.1. Case 1: fully mixed tank

A fully mixed tank is heated up by the serpentine with the inner fluid at a constant inlet temperature. Experimental results and details of the test procedure are reported by Farrington et al. (1986). The test starts with the storage tank with an initial temperature of $T_{ini}^{tnk} = 25^{\circ}C$. Then, fluid at $T_{in}^{hx} = 70^{\circ}C$ is circulated through the serpentine (inlet temperature), until the temperature difference between the inlet and outlet of the serpentine is below $0.1^{\circ}C$. The test was performed under different flow rates through the serpentine of 5, 10 and 15 l/min respectively.

Comparison of numerical and experimental results are shown in Fig. 3. The serpentine effectiveness ϵ , the overall heat transfer coefficient UA^{hx} and the heat exchanger power \dot{Q}^{hx} are analysed as a function of the logarithmic mean temperature difference $LMTD$ during the whole test period.

The instantaneous logarithmic mean temperature $LMTD$ is defined as:

$$LMTD = \frac{T_{in}^{hx} - T_{out}^{hx}}{\ln \frac{T_{in}^{hx} - T_{tnk}}{T_{out}^{hx} - T_{tnk}}} \quad (19)$$

1
2
3
4
5
6
7
8
9 where T_{in}^{hx} and T_{out}^{hx} refer to inlet and outlet temperature in the immersed
10 heat exchanger and T^{tnk} the temperature of the fully mixed tank.

11 The instantaneous effectiveness of the heat exchanger is defined by:

$$12 \quad \epsilon = \frac{T_{in}^{hx} - T_{out}^{hx}}{T_{in}^{hx} - T^{tnk}} \quad (20)$$

13
14
15
16
17 and the overall heat transfer coefficient UA^{hx} as:

$$18 \quad UA^{hx} = \frac{\dot{Q}^{hx}}{LMTD} \quad (21)$$

19
20
21
22
23 where the \dot{Q}^{hx} is the total heat exchanger heat flux in [W].

24 Numerical results are in very good agreement with experimental data
25 for all flow rates and over all the $LMTD$ range. Differences observed be-
26 tween experimental and numerical curves of ϵ , UA^{hx} and \dot{Q}^{hx} for a specific
27 $LMTD$ value are always kept below 5 %, while the statistical error of the
28 experimental data as presented in Fig. 3 are also in the range of $\pm 5\%$.

29 This case permits the validation of the immersed serpentine model under
30 heating mode, however, no tank cooling process is tested. Furthermore, as a
31 fully mixed tank is assumed by using a single node, the reversion elimination
32 algorithm is neither validated. The validation of these two concepts is carried
33 out with the test case 2 in the following subsection.

34 *3.2. Case 2: stratified tank with inverse temperature gradients*

35 The tank energy is varied by setting the inlet serpentine temperature in
36 a series of four pulses so as the serpentine acts both heating and cooling the
37 tank. A high level of stratification is assumed. As inverse temperature gra-
38 dients occur, the reversion elimination algorithm is here necessary. This case
39 is extracted from the work reported by Mather et al. (2002). In this report
40 experimental and numerical results analysing the performance of single and
41 multi-tanks with internal serpentine heat exchangers are presented. Further
42 details on the tank technical data and testing conditions can be found there.

43 Values of the multi-node tank model parameters N , Λ and UA^{tnk} , together
44 with additional tuning parameters to account for the effect of the serpentine
45 were also experimentally obtained and reported by Mather et al. (2002). The
46 tank model here reported differs from the model adopted by Mather et al.
47 (2002) on the use of the energy conservative reversion elimination algorithm

1
2
3
4
5
6
7
8
9 and the detailed modelling of the serpentine. As a result, only the tuning pa-
10 rameters of the multi-node model, i.e. N , Λ and UA^{tnk} are required. Results
11 here presented make use of the multi-node model parameters determined by
12 Mather et al. (2002), see Table 2.
13

14 The tank is modelled with $N = 21$ nodes and using a value of the equiv-
15 alent conductivity coefficient Λ of 1.3 times the thermal conductivity of the
16 tank fluid (water). The nodes are labelled from 1 to 21 starting at the bot-
17 tom. The node 1 is just below the serpentine, and the serpentine is located
18 inside node 2.
19

20 The test starts with the tank at $20^{\circ}C$. Then, water is circulated through
21 the serpentine varying the input temperature T_{in}^{hx} each two hours, taking
22 the value of $40^{\circ}C$, $60^{\circ}C$, $35^{\circ}C$ and $25^{\circ}C$ sequentially. With this test, the
23 serpentine actuates both introducing and removing energy from the tank, and
24 additionally, inverse temperature gradients situations occur that are handled
25 numerically by the reversion elimination algorithm.
26

27 Comparison of the experimental data of Mather et al. (2002) and the
28 results from the numerical model are presented in Fig. 4. Shown are the
29 evolution of the inlet and outlet serpentine temperatures during the 8 hours
30 test period, and the evolution of a selection of the tank nodes temperatures
31 during the test period.
32

33 Again, the numerical results match the experimental data very well for
34 all step change pulses along the time. Some discrepancies are observed in
35 node 1 during the tank heating process taking place within the 4 first hours
36 of the experiment. A similar behaviour was observed in the model used by
37 Mather et al. (2002). During this period, all nodes are heated from below
38 except node 1. Therefore, the reversion elimination algorithm is actuating
39 resulting into a totally mixed tank from node 2 to node 21. On the contrary,
40 node 1 is heated from above, and the model assumes that heat transfer from
41 node 2 to 1 is only due to diffusion. The experiments, however, showed
42 how node 1 was also mixed with other nodes due to the penetration of the
43 convective flows generated at node 2. This aspect is not accounted by the
44 model here described. As concluded by Mather et al. (2002), however, as node
45 1 only constitutes a 5% of the total tank volume, and this effect only occurs
46 during partial periods of the total test, the accuracy of the computed output
47 temperature of the serpentine is not significantly affected. Modifications in
48 the tank multi-node to account this aspect could be included. However, it
49 would introduce additional model complexity that according to the authors
50 concern may not be justified.
51
52
53
54
55
56
57
58

1
2
3
4
5
6
7
8
9 During the last 4 hours of the experiment, the serpentine inlet temper-
10 ature is below the tank nodes temperature. The reversion elimination algo-
11 rithm actuates mixing the nodes 1 and 2. Heat transfer between other nodes
12 is dominated by diffusion. Numerical results show very good agreement with
13 the experimental values.
14
15

16 17 **4. Conclusions** 18

19 A model for thermal storage tanks with internal serpentine heat exchanger
20 has been developed and presented in this work. The model combines the
21 use of the standard multi-node approach for storage tanks, with a reversion
22 elimination algorithm based on energy conservation, and a one-dimensional
23 control volume approach for the fluid flow through the serpentine.
24

25 The use of the energy conservative reversion elimination algorithm re-
26 sults into a simple and consistent formulation that avoids unrealistic inverse
27 temperature gradient solutions in the multi-node, while preserving energy
28 conservation in all tank nodes and, therefore, in the whole tank. According
29 to author's experience, conservative models in systems simulations improve
30 convergence and robustness of the results. Additionally, programming as-
31 pects as identification of bugs and code verification are also facilitated.
32

33 The one dimensional control volume based model for the serpentine min-
34 imizes the required input technical data of the serpentine. Only with the
35 geometrical parameters diameter, length and wall thickness it is possible to
36 accurately evaluate its performance. Furthermore, with an appropriate for-
37 mulation of the heat transfer and fluid flow governing equations, it may be
38 possible to handle more complex physical phenomena inside the serpentine,
39 like coupling of the serpentine in a thermosyphone loop, or two phase fluid
40 flow.
41

42 The model has been validated under two test cases reported in the liter-
43 ature. These tests involve diverse working conditions as heating and cooling
44 process of the tank through the serpentine, and inverse temperature gradi-
45 ents. Input values used for the computation were standard input data for the
46 multi-node model and geometric data for the serpentine, with no need of spe-
47 cific performance data of the heat exchanger nor specific tuning of additional
48 parameters for the heat exchanger.
49
50
51
52
53
54
55
56
57
58

1
2
3
4
5
6
7
8
9 **Nomenclature**

10 A area (m^2); algebraic coefficient in Eq. 8
11 A_F fitting coefficient in Eq. 16
12 B algebraic coefficient in Eq. 8
13 C fitting coefficient in Eq. 13
14 C_F fitting coefficient in Eq. 16
15 C_N fitting coefficient in Eq. 17
16 CV_s control volumes
17 c_p specific heat at constant pressure (J/kgK)
18 D diameter (m)
19 Exp experimental
20 Gr Grashof number
21 Gz Graetz number
22 h heat transfer coefficient (W/m^2K)
23 K fitting coefficient in Eq. 13
24 L total serpentine length (m)
25 $LMTD$ logarithmic mean temperature difference ($^{\circ}C$)
26 M total number of control volumes used in the serpentine
27 \dot{m} mass flow rate (kg/s)
28 N total number of nodes used in the multi-node model
29 n_N fitting coefficient in Eq. 17
30 Num numerical
31 Nu Nusselt number
32 Pr Prandtl number
33 \dot{Q} heat (W)
34 Re Reynolds number
35 S surface (m^2)
36 T temperature ($^{\circ}C$)
37 UA overall heat transfer coefficient (W/K)
38 V volume (m^3)
39 β volumetric coefficient of thermal expansion ($1/K$)
40 Δt time increment (s)
41 δ distance (m)
42 ϵ heat exchanger effectiveness
43 κ conductance (W/m^2K)
44 Λ equivalent conductivity coefficient (W/mK)
45 λ thermal conductivity (W/mK)
46 ρ density (kg/m^3)
47 μ dynamic viscosity (kg/sm)

1
2
3
4
5
6
7
8
9
10
11
12
13
14
15
16
17
18
19
20
21
22
23
24
25
26
27
28
29
30
31
32
33
34
35
36
37
38
39
40
41
42
43
44
45
46
47
48
49
50
51
52
53
54
55
56
57
58
59
60
61
62
63
64
65

Subscripts

ext external
in at inlet
ini initial conditions
int internal
m control volume index in the serpentine model
n node index in the tank multi-node model
out at outlet

Superscripts

a ambient
acum accumulated heat
col collector
F forced convection
hx heat exchanger
load referred to heat load
loss referred to heat loss
m fitting coefficient in Eq. 13
mix mixing
N natural (free) convection
n fitting coefficient in Eq. 13
o value at the previous time step
tnk tank
wall referred to wall

1
2
3
4
5
6
7
8
9 **References**

- 10
11 Banister, Carsen J., Wagar, William R. and Collins, Prof. Michael R., 2014.
12 Validation of a single tank, multi-mode solar-assisted heat pump TRNSYS
13 model. *Energy Procedia* 48 (2014), 499-504.
14
- 15
16 Campos Celador, A., Odriozola, M. and Sala, J.M., 2011. Implications of
17 the modelling of stratified hot water storage tanks in the simulation of the
18 CHP plants. *Energy Conversion and Management*, 52 (2011), 3018-3026.
19
- 20
21 Carbonell, D., Cadafalch, J. and Consul, R., 2013. Dynamic modelling of flat
22 plate solar collectors. *Solar Energy*, 89, 100-112.
23
- 24
25 Churchill, S.W., 2002. Combined free and forced convection around immersed
26 bodies. *Heat Exchanger Design handbook*, Hewitt G.F., sec. 2.5.9. Hemi-
27 sphere Publishing Corporation.
- 28
29 Consul, R., Rodríguez, I., Pérez-Segarra, C.D., and Oliva, A., 2004. Virtual
30 prototyping of storage tanks by means of three-dimensional cfd and heat
31 transfer numerical simulations. *Solar Energy*, 77, 179-191.
32
- 33
34 Drück, H., 1994. Weiterentwicklung und validierung des modells für solare
35 Warmwasserspeicher für das simulationsprogramm TRANSYS. Diplomar-
36 beit ITW, Universität Stuttgart.
- 37
38 EN 12977-3, 2012. European Standard. Thermal solar systems and compo-
39 nents - Custom built systems - Part 3: Performance test methods for solar
40 water heater stores European Committee for Standardisation.
41
- 42
43 Farrington, R.B. and Bingham , C.E., 1986. Analysis of Immersed heat ex-
44 changers, Solar Energy Research Institute, Golden, CO.
- 45
46 Furbo, S., 2003. Optimum design of small DHW low flow solar heating sys-
47 tems. In *Proceedings, ISES solar World Congress, Budapest, Hungary*.
48
- 49
50 Kleinbach, E.M., Beckman, W.A. and Klein, S.A., 1993. Performance study
51 of one-dimensional models for stratified thermal storage tanks. *Solar En-
52 ergy*, 50 (2), 155-166.
53
- 54
55 Mather, D.W., Hollands, K.G.T and Wright J.L., 2002. Single and multi-tank
56 energy storage for solar heating systems: fundamentals. *Solar Energy*, 73
57 (1), 3-13.
58

1
2
3
4
5
6
7
8
9
10
11
12
13
14
15
16
17
18
19
20
21
22
23
24
25
26
27
28
29
30
31
32
33
34
35
36
37
38
39
40
41
42
43
44
45
46
47
48
49
50
51
52
53
54
55
56
57
58
59
60
61
62
63
64
65

Newton, B.J., Schmid M., Michell J.W. and Beckman, W.A., 1995. Storage tank models. Proceedings of ASME/JSME International Solar Energy Conference, March 19-24, 1995. Maui, Hawaii. American Society of Mechanical Engineers, New York, 2 , 1111-1116.

Patankar, S.V., 1980. Numerical heat transfer and fluid flow. Hemisphere.

Savicki, Darci L., Vilemo, Horcio A. and Krenzinger, A., 2011. Three-dimensional analysis and investigation of the thermal and hydrodynamic behaviours of cylindrical storage tanks. Renewable Energy 36 (2011), 1364-1373.

Shah, L.J., 2000. Heat transfer correlations for vertical mantle heat exchangers. Solar Energy, 96, 157-171.

Shuhong Li, Yongxin Zhang, Kai Zhang, Xianliang Li, Yang Li and Xiaosong Zhang, 2014. Study on performance of storage tanks in solar water heater system in charge and discharge progress. Energy Procedia 48 (2014), 384-393.

Wong, H.Y., 1977. Handbook of essential formulae and data on heat transfer for engineers. Longman Group Limited London.

Yan Su and Davidson, Jane H., 2008. Discharge of thermal storage tanks via immersed baffled heat exchangers: numerical model of flow and temperature fields. J. Sol. Energy Eng., 130 (2), doi:10.1115/1.2856012

Young-Deuk Kim, Kyaw Thu, Hitasha Kaur Bhatia, Charanjit Singh Bhatia and Kim Choon Ng, 2012. Thermal analysis and performance optimization of a solar hot water plant with economic evaluation. Solar Energy, 86 (5), 1378-1395.

1
2
3
4
5
6
7
8
9
10
11
12
13
14
15
16
17
18
19
20
21
22
23
24
25
26
27
28
29
30
31
32
33
34
35
36
37
38
39
40
41
42
43
44
45
46
47
48
49
50
51
52
53
54
55
56
57
58
59
60
61
62
63
64
65

Table 1: Forced convective heat transfer of fluid flow through a cylindrical tube. Experimental fitting parameters in terms of the operating conditions, Wong (1977). The Graetz number Gz is defined as $Gz = (\pi D_{int}/4L) Re Pr$, and L is the total serpentine length.

Operating conditions	C	m	n	K
Laminar flow short tube $Re \leq 2000, Gz > 10$	1.86	1/3	1/3	$(D_{int}/L)^{1/3}$
Laminar flow long tube $Re \leq 2000, Gz < 10$	3.66	0	0	1
Turbulent flow $Re > 2000$	0.027	0.8	0.33	1

1
2
3
4
5
6
7
8
9
10
11
12
13
14
15
16
17
18
19
20
21
22
23
24
25
26
27
28
29
30
31
32
33
34
35
36
37
38
39
40
41
42
43
44
45
46
47
48
49
50
51
52
53
54
55
56
57
58
59
60
61
62
63
64
65

Table 2: Values of the tuning parameters used in the test cases. *) Thermal conductivity of the tank fluid (water).

Case	N	Λ	UA^{tnk}	C_N	n_N
	-	[W/mK]	[W/K]	-	-
1	1	-	1.600	0.5	0.25
2	21	$1.3\lambda^*$	0.569	0.5	0.25

1
2
3
4
5
6
7
8
9
10
11
12
13
14
15
16
17
18
19
20
21
22
23
24
25
26
27
28
29
30
31
32
33
34
35
36
37
38
39
40
41
42
43
44
45
46
47
48
49
50
51
52
53
54
55
56
57
58
59
60
61
62
63
64
65

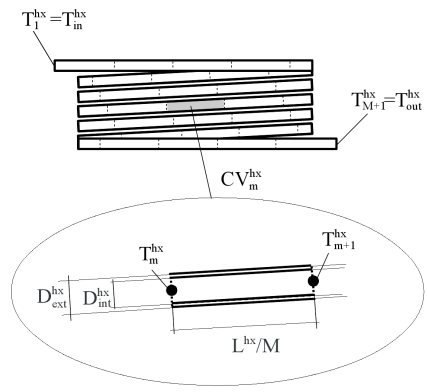


Figure 1: Discretization of a smooth coil serpentine.

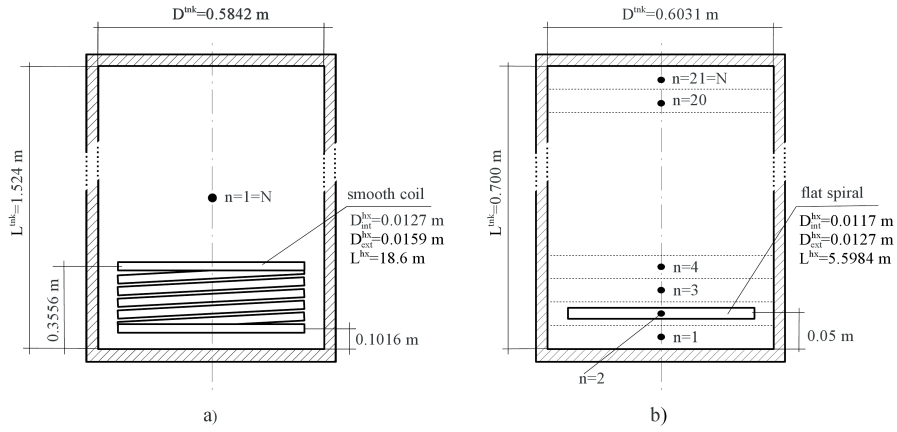


Figure 2: Geometry and tank discretization of the case studies. a) Case 1: fully mixed tank. b) Case 2: stratified tank.

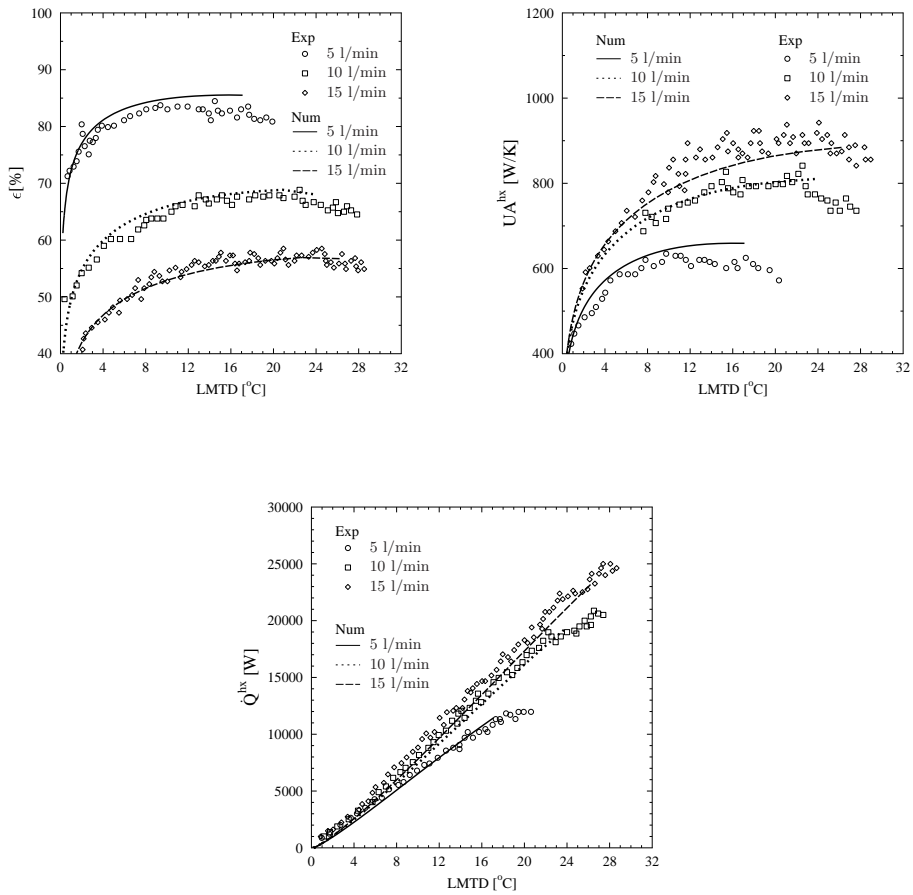


Figure 3: Case 1: fully mixed tank. Immersed heat exchanger efficiency ϵ , heat transfer coefficient UA^{hx} and power \dot{Q}^{hx} along the $LMTD$. Comparison between numerical results and experimental data from Farrington et al. (1986).

1
2
3
4
5
6
7
8
9
10
11
12
13
14
15
16
17
18
19
20
21
22
23
24
25
26
27
28
29
30
31
32
33
34
35
36
37
38
39
40
41
42
43
44
45
46
47
48
49
50
51
52
53
54
55
56
57
58
59
60
61
62
63
64
65

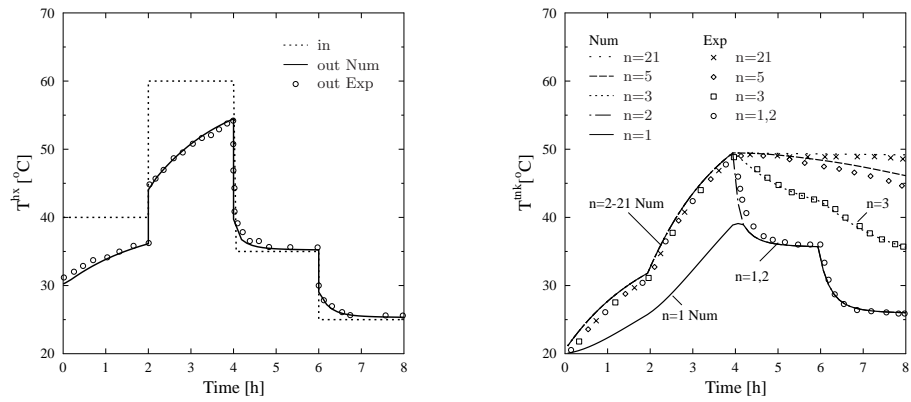


Figure 4: Case 2: stratified tank. Outlet fluid temperature of the immersed heat exchanger and tank temperature for different nodes along time. Comparison between numerical results and experimental data from Mather et al. (2002).